OFC 2018, San Diego, 12th March 2018 – Paper M1G.1

Flexible Transceivers and the Rate/Reach Trade-off

Gabriella Bosco

Politecnico di Torino – Department of Electronics and Telecommunications, Italy

OptCom group – www.optcom.polito.it

Acknowledgments

OptCom Group (PoliTO & ISMB)

- L. Bertignono
- M. Cantono
- A. Carena
- V. Curri
- R. Gaudino
- F. Guiomar
- A. Nespola
- D. Pilori
- P. Poggiolini
- …

CISCO

- A. Bisplinghoff
- T. Duthel
- C. Fludger
- F. Forghieri
- …

- J. Fischer
- C. Laperle
- N. Nelson
- D. Plant
- K. Roberts
- C. Schubert
- P. Winzer
- X. Zhou
- ….

ISMB Istituto Superiore Mario Boella

CISCO

OPTCOM

Introduction

- What are **flexible transceivers** and why are they needed?
- Transceivers that enable operation at one of **multiple data rates**, by changing at least one parameter such as the modulation format, symbol rate or number of subcarriers used for an aggregate channel.
- Flexibility realized using a **common, fixed hardware configuration**, with functionality selected via software commands.
- Motivations:
  - Same transceiver can be used for different applications
  - Increased efficiency in network planning
  - Better exploitation of available resources

→ **Reduction of costs**

Historical evolution of data rates

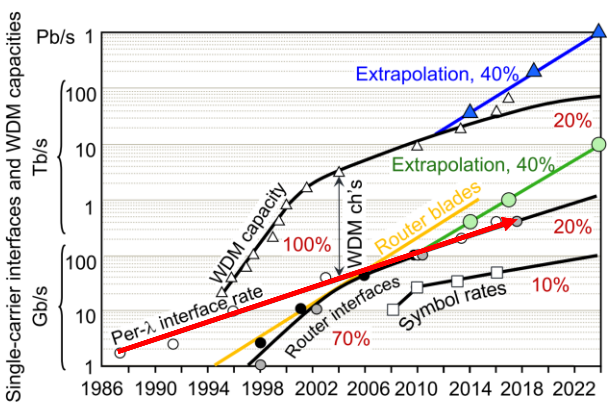

Winzer et al., JLT vol. 35, p. 1099, 2017

Historical evolution of data rates

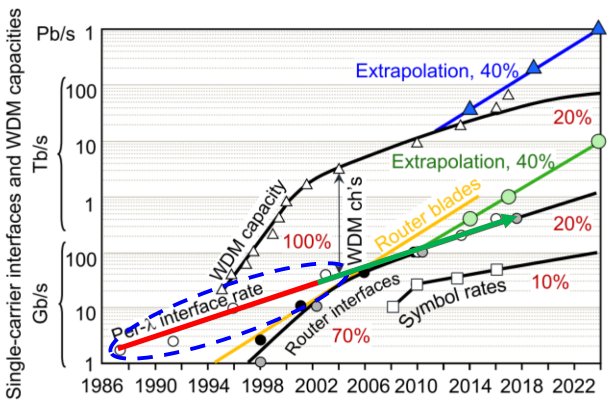

Winzer et al., JLT vol. 35, p. 1099, 2017

- WDM with EDFA amplifiers
  - ~5 THz available in the C-band
  - ~100 channels with 50 GHz spacing
- Legacy **direct-detection** systems → low level of flexibility
  - Different hardware required for binary and multi-level formats
  - Transmission reach increased using optical dispersion management

The "Coherent Revolution"

- Increased Transmission Rate
  - High-order modulation formats (data rate x number of bits per symbol)
  - Polarization-multiplexing (x 2 in transmission rate)
  - Spectral shaping → reduced frequency spacing can be tolerated → potential increase in spectral efficiency (SE) and data rate

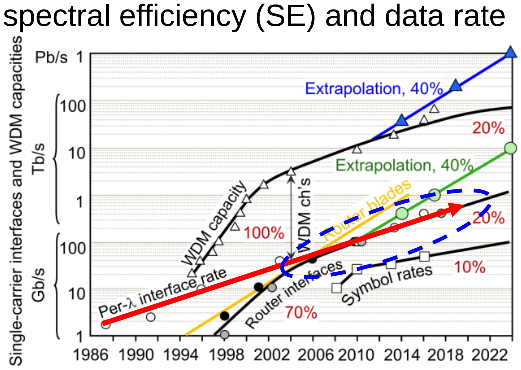

The “Coherent Revolution”

- Increased Transmission Rate
  - High-order modulation formats (data rate x number of bits per symbol)
  - Polarization-multiplexing (x 2 in transmission rate)
  - Spectral shaping → reduced frequency spacing can be tolerated → potential increase in spectral efficiency (SE) and data rate
- Increased Reach
  - DSP algorithms for linear and nonlinear system impairments compensation
  - Energy-efficient and nonlinearity-tolerant modulation formats
- Increased Flexibility
  - Same hardware can be used to generate and detect different modulation formats
  - No dispersion management needed
  - Adaptive modulation techniques with fine granularity

Outline

1. Coherent transceivers architecture
2. Digital signal processing (DSP) algorithms
3. Standard QAM modulation formats
   - Rate/reach trade-off
   - Flexibility
4. Advanced modulation techniques
   - Subcarrier multiplexing (SCM)
   - Time-domain hybrid formats (TDHF)
   - Multi-dimensional modulation formats
   - Probabilistic shaping (PS)
5. Modulation format independent DSP algorithms

1) Coherent transceivers architecture

Dual-Polarization Coherent Transceiver

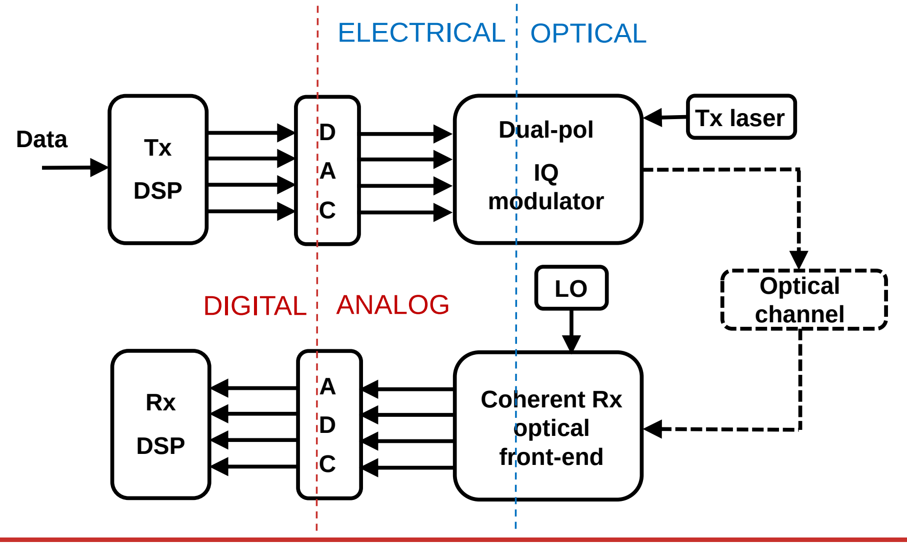

Dual-polarization IQ modulator

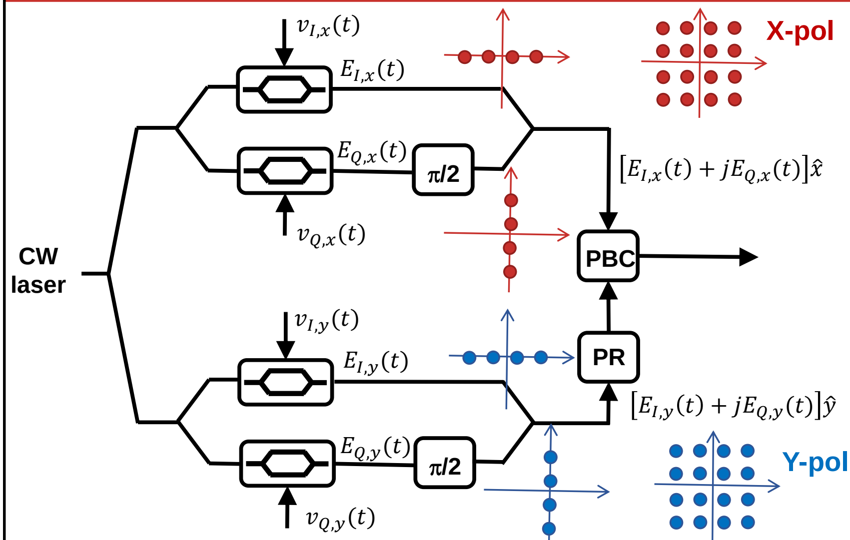

- PBC: polarization beam combiner
- PR: polarization rotator
- $v_{I,x}(t)$, $v_{Q,x}(t)$: in-phase and quadrature component of the driving signal for x-pol
- $v_{I,y}(t)$, $v_{Q,y}(t)$: in-phase and quadrature component of the driving signal for y-pol

Coherent Rx Optical Font-End

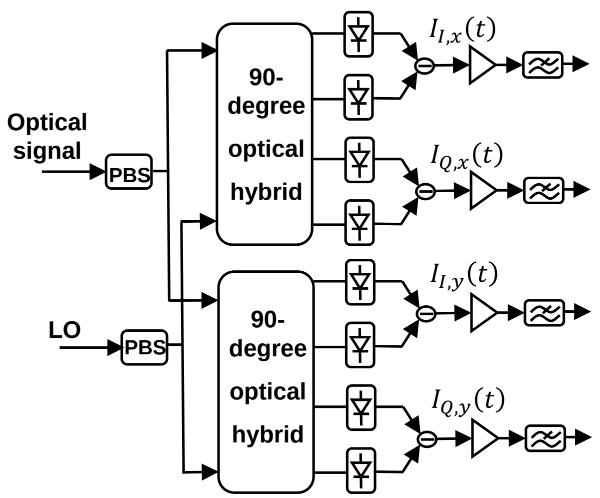

$$I_{IQ}(t) = I_I(t) + jI_Q(t)$$
$$= 4R\sqrt{P_S(t)P_{LO}}e^{j(2\pi\delta f t + \phi_D(t) - \phi_{LO}(t))}$$

- $P_S(t)$: power of the optical signal
- $\phi_D(t)$: phase of the optical signal
- P_{LO}: LO power
- $\phi_{LO}(t)$: LO phase noise
- δf: frequency offset between optical signal and LO

PBS: polarization beam splitter

DAC – Sampling speed

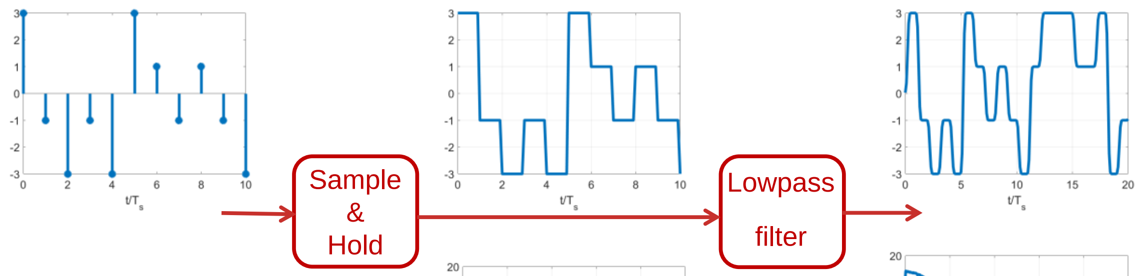

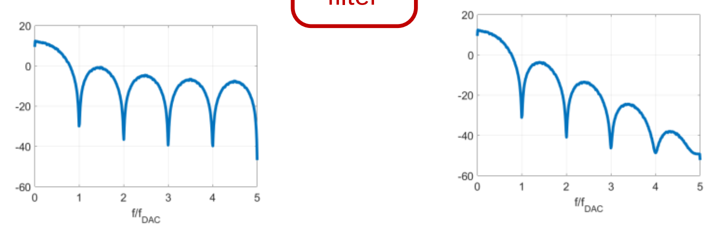

- f_{DAC} = DAC speed (in samp/s)
- T_s= symbol time
- Maximum symbol rate: f_{DAC} → **1 samp/symb**
  - BUT **no shaping possible!**

Sample & hold + filter can be compensated for by DSP

DAC – Resolution

- **Maximum number of modulation levels limited by number of resolution bits**

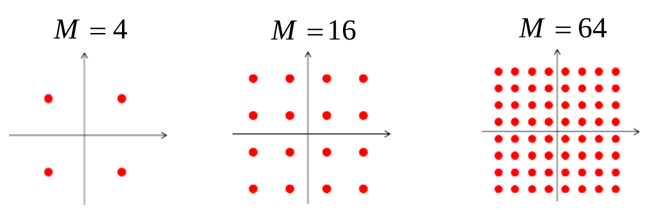

- Minimum number of bits @ 1 samp/symb: $\log_2\left(\sqrt{M}\right)$
- Required number of bits @ 2 samp/symb: $\sim \log_2\left(\sqrt{M}\right)+3$

Pfau, JLT, vol. 27, p. 989, 2009

ADC – Sampling speed

- In order to avoid a performance degradation due to *aliasing,* the ADC sampling frequency f_{ADC} has to be higher than twice the bandwidth of the input signal.
  - An **additional antialiasing electrical filter** may be needed before the ADC in order to reduce the bandwidth of the input signal.
  - The distortions introduced on the useful signal by the bandwidth limitations of the Rx can be compensated for in the digital domain by the adaptive or static equalizers present in the DSP chain.

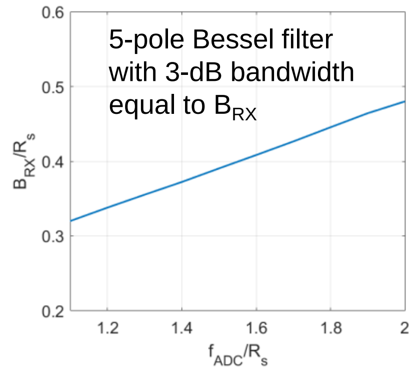

Tx laser and LO – Laser linewidth

- Phase noise can be modeled as a Wiener process: $\phi_k = \sum_{i=-\infty}^{k} f_i$
  - the f_i's are independent and identically distributed random Gaussian variables with zero mean and variance $\sigma_f^2 = 2\pi\,\Delta\nu\cdot T_s$
  - $\Delta\nu$ is the sum linewidth of Tx laser and local oscillator
  - T_s is the symbol period.
- **High-order formats are more impacted by phase noise**

Modulation format	Maximum tolerable $\Delta\nu\cdot T_s$	Maximum tolerable $\Delta\nu$ @ 10 Gbaud	Maximum tolerable $\Delta\nu$ @ 32 Gbaud	Maximum tolerable $\Delta\nu$ @ 64 Gbaud
QPSK	$4.1\cdot10^{-4}$	4.1 MHz	13.1 MHz	26.2 MHz
16-QAM	$1.4\cdot10^{-4}$	1.4 MHz	4.5 MHz	9.0 MHz
64-QAM	$4.0\cdot10^{-5}$	400 kHz	1.3 MHz	2.6 MHz
256-QAM	$8.0\cdot10^{-6}$	80 kHz	256 kHz	512 kHz

Pfau, JLT, vol. 27, p. 989, 2009

2) Digital signal processing algorithms

Transmitter DSP

- Spectral shaping to increase SE→ Nyquist-WDM

Spectral efficiency (SE)

$$SE = n_{bps} \cdot \frac{R_s}{\Delta f} \cdot r_{FEC} = \frac{n_{bps} \cdot r_{FEC}}{\delta f} \quad \text{[bit/symb]} \qquad \delta f = \frac{\Delta f}{R_s}$$

- Pre-compensation of bandwidth limitations
- Pre-compensation of Mach-Zehnder modulator non-linear transfer function
- Pre-compensation of propagation effects: CD and/or nonlinear interference (NLI)

Savory, Elec. Lett., vol. 42, p.407, 2006
Kamio et al., LEOS, p. MC1.2, 2008
Ghazisaiedi et al., ECOC, p. We.4.D.4, 2013
Rafique et al., JLT, vol. 33, p. 140, 2015
Khanna et al., PTL, vol. 28, p.752, 2016
Berenguer et al., JLT, vol. 34, p.1739, 2016
Roberts et al., JOCN, vol. 9, p. C12, 2017

High SE modulation: Nyquist-WDM

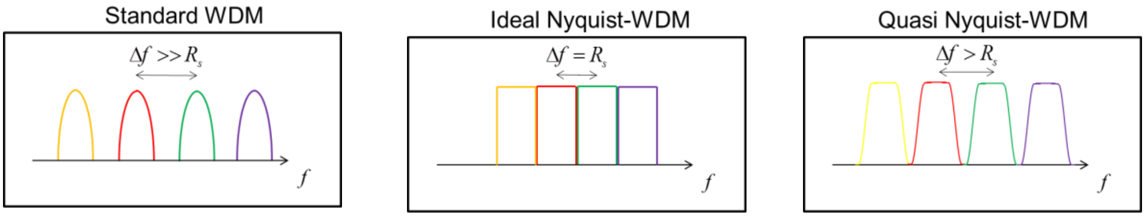

- Maximum information that can be transmitted by the WDM comb:

$$R_b^{tot} = SE \cdot B_{WDM} = $$
$$= n_{bps} \cdot \frac{R_s}{\Delta f} \cdot B_{WDM} \cdot r_{FEC} = $$
$$= n_{bps} \cdot \frac{B_{WDM}}{\delta f} \cdot r_{FEC}$$

$$\delta f = \frac{\Delta f}{R_s}$$

B_{WDM}: total bandwidth of the WDM comb
r_{FEC}: rate of the FEC code
n_{bps}: number of bits per symbol

Generation of a Nyquist-WDM signal

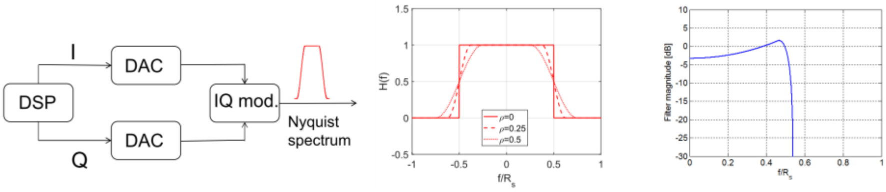

shaping filter

$$R_s = \frac{f_{DAC}}{N_{SpS}}$$

DAC sampling speed (samp/s)
Number of samples per symbol

- R_s can be increased by reducing the "oversampling factor" N_{SpS} → interference between spectral replica → need to use a **proper anti-alias filter**

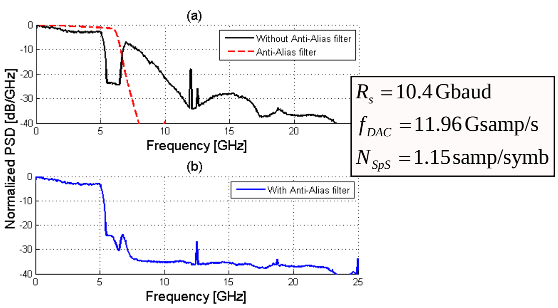

Nespola et al., Opt. Exp., vol. 22, p.1796, 2014

Receiver DSP – Block diagram

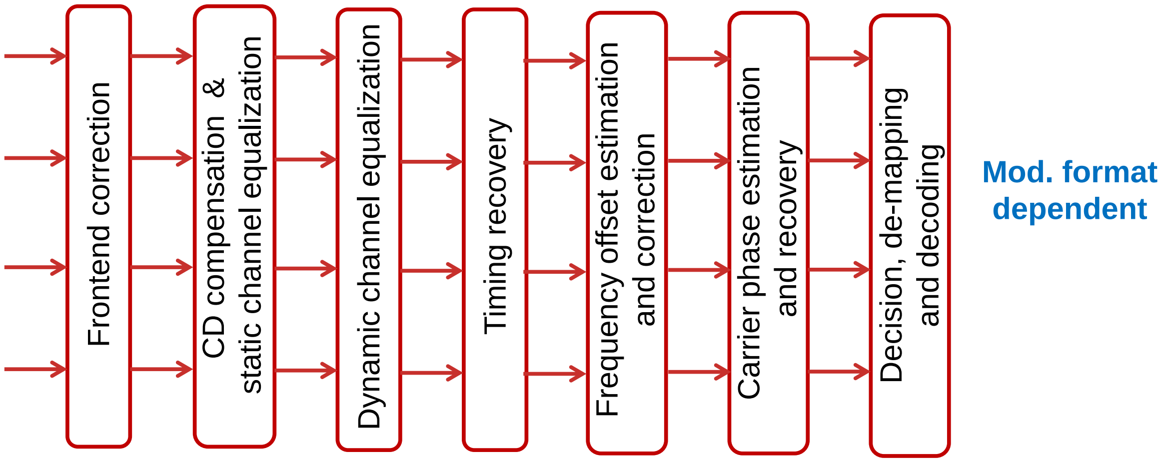

Kuschnerov et al., JLT, vol. 27, p. 3614, 2009

Savory, JSTQE, vol. 16, p. 1164, 2010

Adaptive equalizer

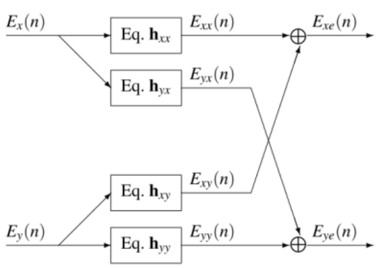

$$E_{xe}(n) = \mathbf{E}_x^T \mathbf{h}_{xx} + \mathbf{E}_y^T \mathbf{h}_{xy}$$
$$E_{ye}(n) = \mathbf{E}_x^T \mathbf{h}_{yx} + \mathbf{E}_y^T \mathbf{h}_{yy}$$

- Update of the equalizer weights based on the minimizations of error signals using the stochastic gradient algorithm.

Constant modulus algorithm (CMA)

$$h_{xx} = h_{xx} + \mu\varepsilon_x E_x E_{xe}^*$$
$$h_{xy} = h_{xy} + \mu\varepsilon_x E_y E_{xe}^*$$
$$h_{yx} = h_{yx} + \mu\varepsilon_y E_x E_{ye}^*$$
$$h_{yy} = h_{yy} + \mu\varepsilon_y E_y E_{ye}^*$$

$$\varepsilon_x = 1 - |E_{xe}|^2$$
$$\varepsilon_y = 1 - |E_{ye}|^2$$

Savory, Opt. Exp., vol. 16, p. 804, 2008

Least mean square (LMS)

$$h_{xx} = h_{xx} + \mu\varepsilon_x E_x^*$$
$$h_{xy} = h_{xy} + \mu\varepsilon_x E_x^*$$
$$h_{yx} = h_{yx} + \mu\varepsilon_y E_y^*$$
$$h_{yy} = h_{yy} + \mu\varepsilon_y E_y^*$$

$$\varepsilon_x = d_x - E_{xe}(n)$$
$$\varepsilon_y = d_y - E_{ye}(n)$$

d_x, d_y: constellation points

Carrier phase estimation (CPE)

Viterbi & Viterbi

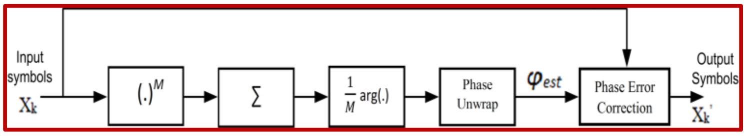

Blind phase search (BPS)

Pfau et al., JLT, vol. 27, p. 989, 2009

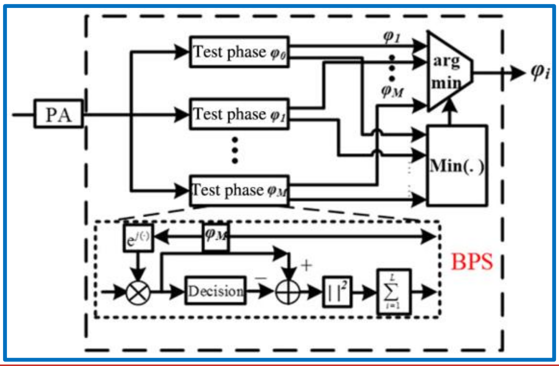

3) Standard PM-QAM modulation formats

Ideal back-to-back performance

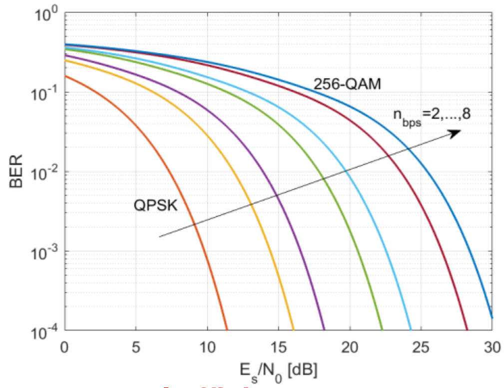

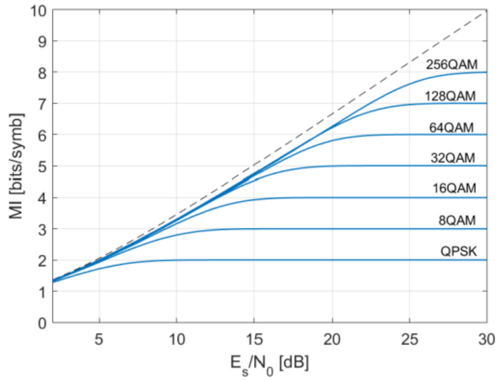

Spectral efficiency

$$SE = n_{bps} \cdot \frac{R_s}{\Delta f} \cdot r_{FEC}$$

- If n_{bps} increases, SE increases but the back-to-back performance gets worse → reduction in reach

Rate/reach trade-off

- Analyzed setup:
  - Nyquist-WDM transmission at R_s = 32 Gbaud, with spacing Δf=1.05 R_s (roll-off 0.05)
  - Bandwidth of the WDM comb: 5 THz
  - SNR margin of 3 dB w.r.t. the ideal back-to-back performance
  - EDFA only amplification with F = 5 dB
  - PSCF or SSMF with 100-km span length

Rate/reach trade-off

- Analyzed setup:
  - Nyquist-WDM transmission at R_s = 32 Gbaud, with spacing Δf=1.05 R_s (roll-off 0.05)
  - Bandwidth of the WDM comb: 5 THz
  - SNR margin of 3 dB w.r.t. the ideal back-to-back performance
  - EDFA only amplification with F = 5 dB
  - PSCF or SSMF with 100-km span length

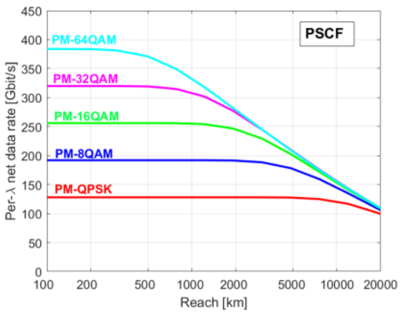

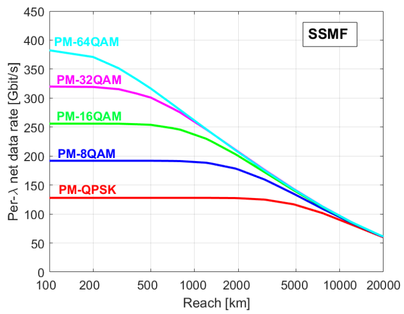

Results obtained using the EGN model

Poggiolini et al., JLT, vol. 35, p. 458, 2017

Rate/reach trade-off

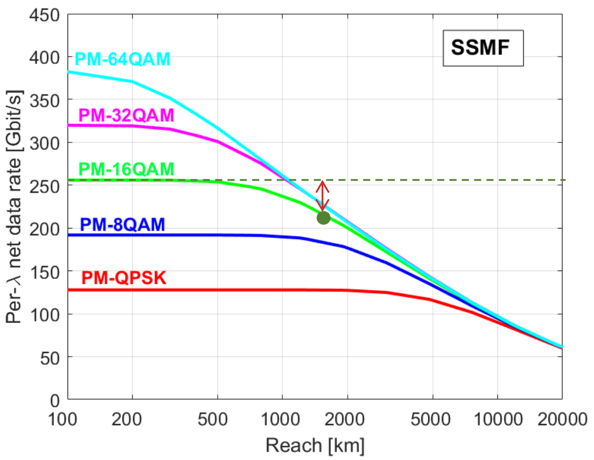

- Distance between the operating point and the asymptotic performance
  → **FEC overhead**

Rate/reach trade-off

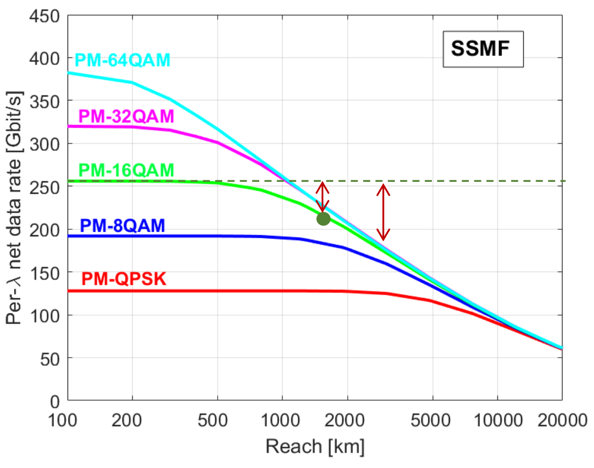

- Distance between the operating point and the asymptotic performance → **FEC overhead**
- Complexity increases with modulation format order and FEC overhead

Flexibility – Adaptive modulation format

$$R_b^{tot} = SE \cdot B_{WDM} =$$
$$= n_{bps} \cdot \frac{R_s}{\Delta f} \cdot B_{WDM} \cdot r_{FEC} =$$
$$= n_{bps} \cdot \frac{B_{WDM}}{\delta f} \cdot r_{FEC}$$

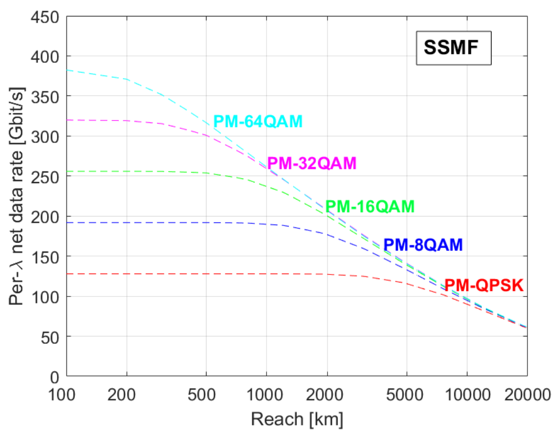

- n_{bps} can be changed only in discrete steps

Flexibility – Adaptive modulation format

$$R_b^{tot} = SE \cdot B_{WDM} =$$
$$= n_{bps} \cdot \frac{R_s}{\Delta f} \cdot B_{WDM} \cdot r_{FEC} =$$
$$= n_{bps} \cdot \frac{B_{WDM}}{\delta f} \cdot r_{FEC}$$

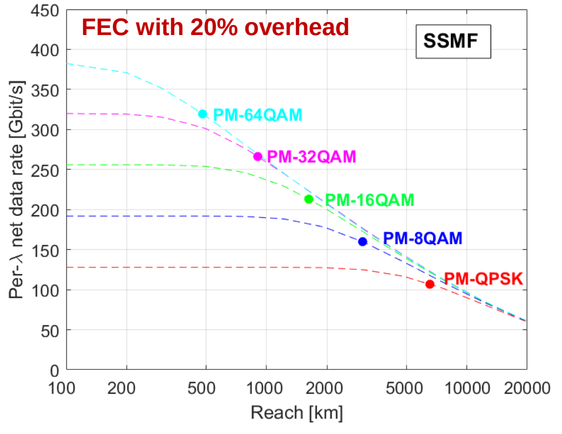

- n_{bps} can be changed only in discrete steps

Flexibility - Adaptive code rate

$$R_b^{tot} = SE \cdot B_{WDM} =$$
$$= n_{bps} \cdot \frac{R_s}{\Delta f} \cdot B_{WDM} \cdot r_{FEC} =$$
$$= n_{bps} \cdot \frac{B_{WDM}}{\delta f} \cdot r_{FEC}$$

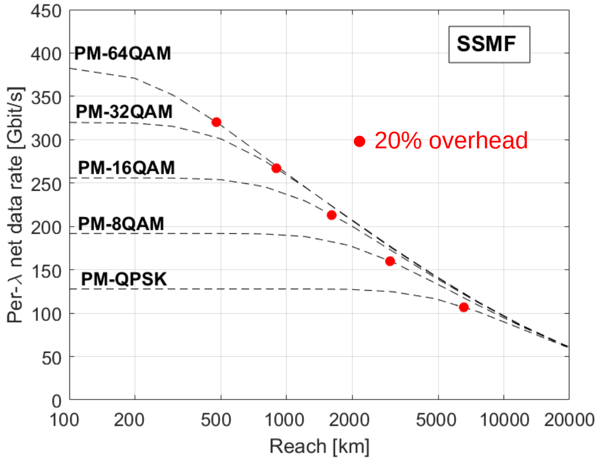

Flexibility - Adaptive code rate

$$R_b^{tot} = SE \cdot B_{WDM} = n_{bps} \cdot \frac{R_s}{\Delta f} \cdot B_{WDM} \cdot r_{FEC} = n_{bps} \cdot \frac{B_{WDM}}{\delta f} \cdot r_{FEC}$$

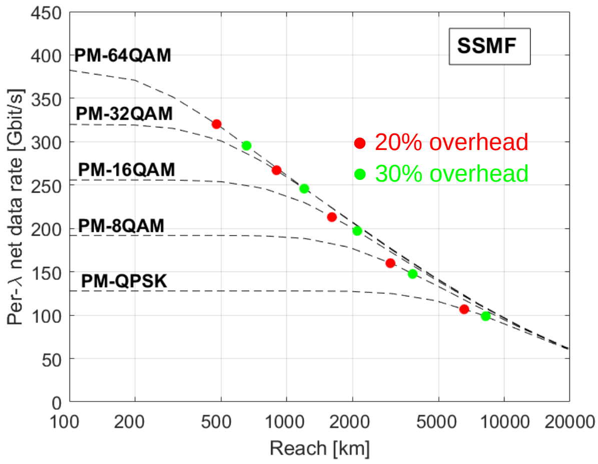

Flexibility - Adaptive code rate

$$R_b^{tot} = SE \cdot B_{WDM} = n_{bps} \cdot \frac{R_s}{\Delta f} \cdot B_{WDM} \cdot r_{FEC} = n_{bps} \cdot \frac{B_{WDM}}{\delta f} \cdot r_{FEC}$$

- The required hardware effort for implementation of several FEC encoders and decoders in order to support the various code rates is significant and may lead to an undesired increase of transceiver cost

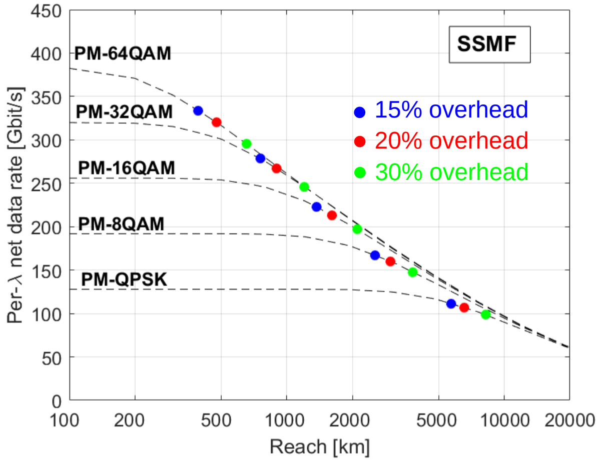

Zhou, Comm. Mag., vol. 51, p. 41, 2013

4) Advanced modulation techniques

Fixed symbol-rate transceivers

- The analog electronic and optoelectronic parts of a transceiver are usually designed for a specific target symbol rate → it is reasonable to assume that a cost-efficient realization of a flexible transceiver operates at a fixed symbol rate.
- Several approaches exist to realize flexible variation of the three key parameters of a transceiver:
  - spectral efficiency
  - bit rate
  - reach

Most promising approaches:

- Subcarrier multiplexing
- Time-domain hybrid formats
- 4D modulation formats
- Probabilistic shaping

Subcarrier multiplexing

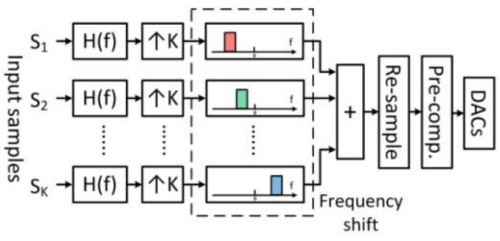

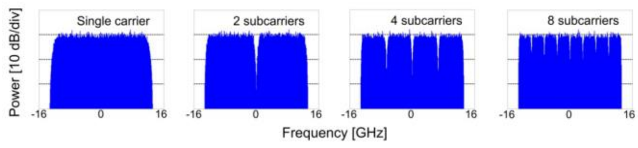

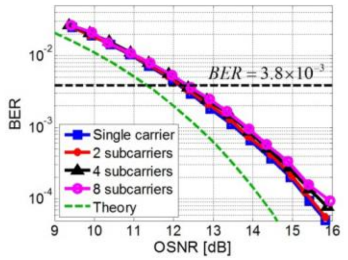

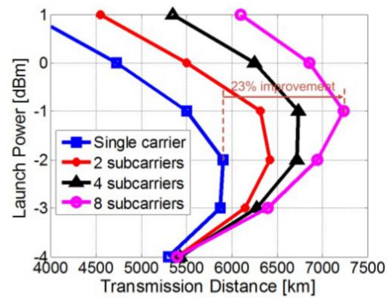

- PM-QPSK
- 24 Gbaud
- roll-off 0.1
- 80-km SMF

Qiu et al., Opt. Exp., vol. 22, p. 18770, 2014

An experimental demonstration

- **19 channel** WDM comb, with channel **spacing 37.5 GHz**, for a total WDM bandwidth of **710 GHz**

P. Poggiolini, JLT, vol. 34, p. 1872, 2016

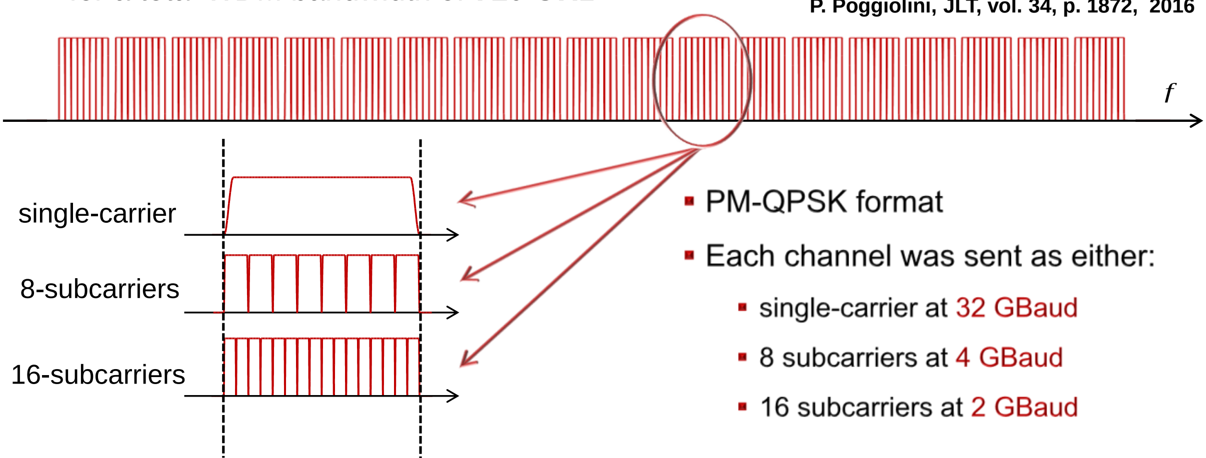

- PM-QPSK format
- Each channel was sent as either:
  - single-carrier at 32 GBaud
  - 8 subcarriers at 4 GBaud
  - 16 subcarriers at 2 GBaud

Reach curves at BER 10^{-2}

- 108-km PSCF, EDFA amplification

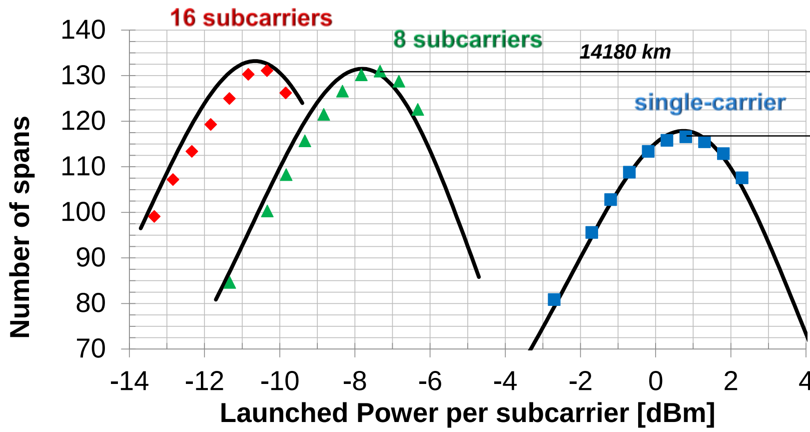

- markers: experiment
- solid lines: EGN model predictions

- 0.1-dB back-to-back penalty from single SC to 16 SCs

P. Poggiolini et al., JLT, vol. 34, p. 1872, 2016

Flexibility

- Increase of system flexibility, by adjusting the number of subcarriers, modulation formats and spectral occupation.

32 Gbaud, 37.5 frequency spacing

QAM order of each SC	Net data rate [Gb/s]	SE [bit/s/Hz]	Max reach [km]
4-4-4-4	100	2.67	1045
4-8-8-4	125	3.33	1045
4-16-16-4	150	4.00	1045
8-8-8-8	150	4.00	665
8-16-16-8	175	4.67	665
16-16-16-16	200	5.33	380

Rahman et al., OFC 2016, p. Tu3K.5

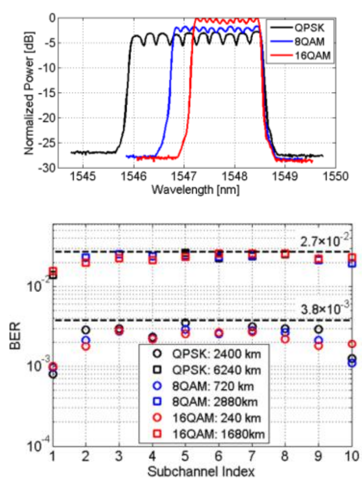

Zhuge et al., Opt. Exp., vol. 22, p. 2278, 2014

Time-domain Hybrid Formats (TDHF)

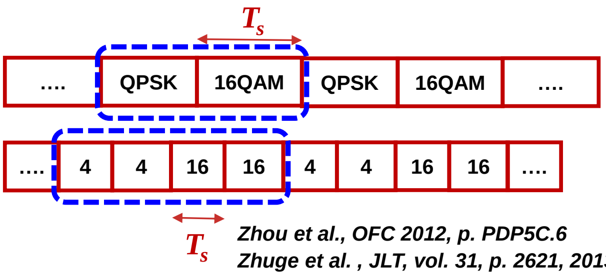

Zhou et al., OFC 2012, p. PDP5C.6
Zhuge et al. , JLT, vol. 31, p. 2621, 2013
Curri et al., OFC 2014, p. Tu3A.2

$$SE = \left(\frac{M_1 N_{b1} + M_2 N_{b2}}{M}\right) \cdot \frac{2R_s}{BW}$$

- $M_{1/2}$ = number of symbols of first/second modulation format in each **TDHF frame**
- M = M_1+M_2= TDHF frame length
- $N_{b1/b2}$ = number of bits per symbol of first/second modulation format
- BW = bandwidth occupancy of the channel
- $P_{1/2}$ = average power of first/second format
- For QPSK: $\Phi(x) = \frac{1}{2}\mathrm{erfc}\left(\sqrt{\frac{SNR}{2}}\right)$

$$BER = \frac{M}{M_1 N_{b1} + M_2 N_{b2}} \left\{ \frac{M_1 N_{b1}}{M} \cdot \Phi_1\left(\frac{MP_1}{M_1 \cdot P_1 + M_2 \cdot P_2} SNR\right) + \frac{M_2 N_{b2}}{M} \cdot \Phi_2\left(\frac{MP_2}{M_1 \cdot P_1 + M_2 \cdot P_2} SNR\right) \right\}$$

Design parameters

- The choice of M_1 and M_2 affects system performance, particularly the tolerance to fiber nonlinearities.
- The power ratio of the two QAM symbols should be optimized to obtain the same BER for the two formats → the power of the lower order QAM should be less than the higher order QAM, since the latter is more sensitive to noise.

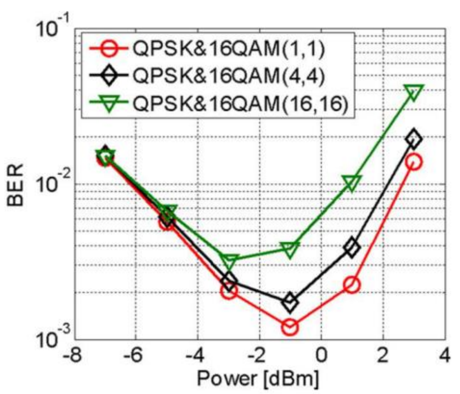

Zhuge et al., JLT, vol. 31, p. 2621, 2013

Flexibility

40 Gbaud, 50 GHz frequency spacing

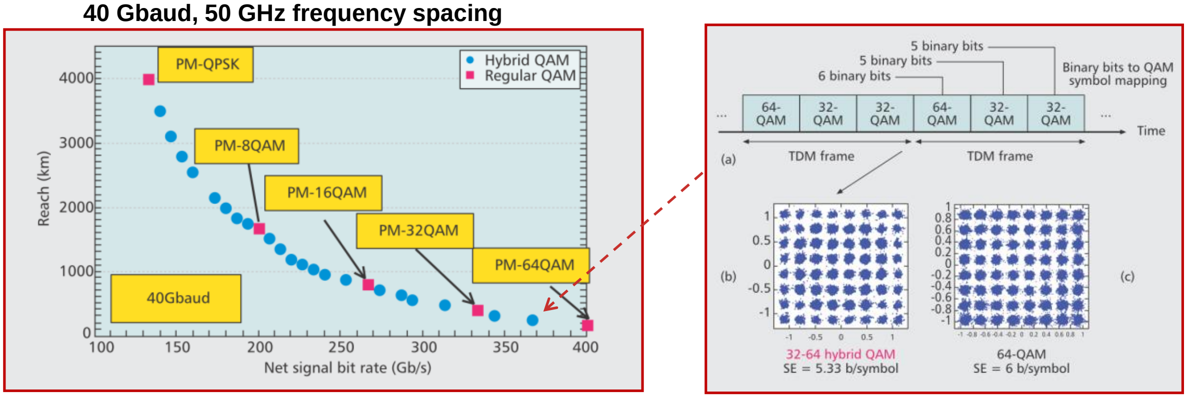

Zhou et al., Comm. Mag., vol. 51, p. 41, 2013

4D modulation formats with set-partitioning

- The idea is to partition the constellation points into smaller subsets that have an increased minimum Euclidean distance and a lower data-rate with respect to the original constellation.
- Advantage: some DSP algorithms designed for standard QAM constellations may be reused.
- Examples:
  - Polarization-switched QPSK (4D constellation composed of 8 points) ***Agrell et al., JLT, vol. 29, p. 5115, 2009***
  - 16QAM set partitioning ***Renaudier et al., OFC 2013, p. OTu3B.1***

PS-QPSK coordinates in the 4D space

- Only one polarization at a time is transmitted → polarization-switched QPSK

$$s_1 = (-2,0,0,0)$$
$$s_2 = (+2,0,0,0)$$
$$s_3 = (0,-2,0,0)$$
$$s_4 = (0,+2,0,0)$$

$$s_5 = (0,0,-2,0)$$
$$s_6 = (0,0,+2,0)$$
$$s_7 = (0,0,0,-2)$$
$$s_8 = (0,0,0,+2)$$

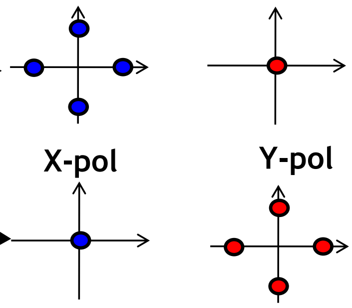

PS-QPSK coordinates in the 4D space

$$s_1 = (-2,0,0,0)$$
$$s_2 = (+2,0,0,0)$$
$$s_3 = (0,-2,0,0)$$
$$s_4 = (0,+2,0,0)$$
$$s_5 = (0,0,-2,0)$$
$$s_6 = (0,0,+2,0)$$
$$s_7 = (0,0,0,-2)$$
$$s_8 = (0,0,0,+2)$$

45° phase rotation ⇒

$$s_1 = \sqrt{2}(-1,-1,0,0)$$
$$s_2 = \sqrt{2}(-1,+1,0,0)$$
$$s_3 = \sqrt{2}(+1,-1,0,0)$$
$$s_4 = \sqrt{2}(+1,+1,0,0)$$
$$s_5 = \sqrt{2}(0,0,-1,-1)$$
$$s_6 = \sqrt{2}(0,0,-1,+1)$$
$$s_7 = \sqrt{2}(0,0,+1,-1)$$
$$s_8 = \sqrt{2}(0,0,+1,+1)$$

45° Polarization rotation ⇒

$$s_1 = (-1,-1,-1,-1)$$
$$s_2 = (-1,-1,+1,+1)$$
$$s_3 = (-1,+1,-1,+1)$$
$$s_4 = (-1,+1,+1,-1)$$
$$s_5 = (+1,+1,+1,+1)$$
$$s_6 = (+1,+1,-1,-1)$$
$$s_7 = (+1,-1,+1,-1)$$
$$s_8 = (+1,-1,-1,+1)$$

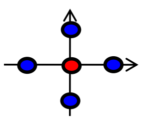

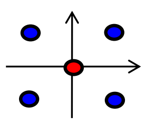

Sub-set of PM-QPSK points

Flexibility

- Reach versus net SE for Nyquist-WDM transmission of selected PM and 4D modulation formats over SSMF at a symbol rate of 32 GBaud assuming SD-FEC with 23% overhead and BER = 2 × 10^{-2} threshold.

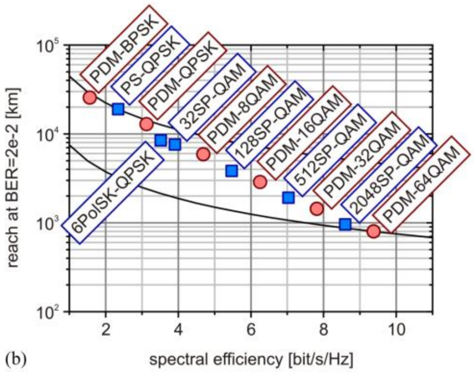

Fischer et al., JLT, vol. 32, p. 2886, 2014

- Solid black lines denote the contours of constant SE × reach products belonging to the best and worst modulation format.

MODULATION FORMATS

Modulation format	Bits per symbol	ROSNR @ 28 GBd [dB][a]	ROSNR @ 32 GBd [dB][b]	Bitrate [Gb/s]
PDM-BPSK	2	9.1	7.4	50
PS-QPSK	3	10.1	8.7	75
PDM-QPSK	4	12.1	10.4	100
6PolSK-QPSK	4.5	13.3	12.2	112
32SP-QAM	5	14.1	12.7	125
PDM-8QAM	6	15.6	13.8	150
128SP-QAM	7	17.1	15.7	175
PDM-16QAM	8	18.7	16.9	200
512SP-QAM	9	20.1	18.7	225
PDM-32QAM	10	21.7	19.8	250
2048SP-QAM	11	23.2	21.7	275
PDM-64QAM	12	24.7	22.6	300

[a] assuming HD-FEC with 7% overhead and a threshold of BER=3.8 × 10^{-3}.
[b] assuming SD-FEC with 23% overhead and a threshold of BER=2 × 10^{-2}.

Probabilistic Shaping (PS)

- PS is based on the transmission of the symbols a_i of a standard QAM constellation with different probabilities in order to approximate the optimum symbol distribution over AWGN channels and thus reduce the QAM shaping loss.

Uniform 64QAM

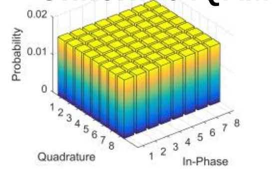

- Using PS, lower-energy (i.e. inner) points of a constellation are transmitted with higher probability.
- Two possible distributions are:

$$P(a_i) = be^{-\lambda |a_i|^2}$$

Buchali et al., JLT, vol. 32, p. 1599, 2015

$$P(a_i) = be^{-\lambda |a_i|}$$

Pilori et al., JLT, vol. 37, p. 501, 2018

PS-64QAM

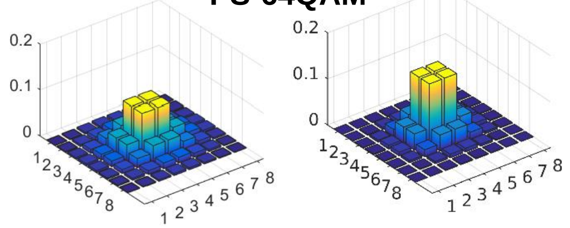

λ =0.46   λ=0.83

Example of generation of PS signals

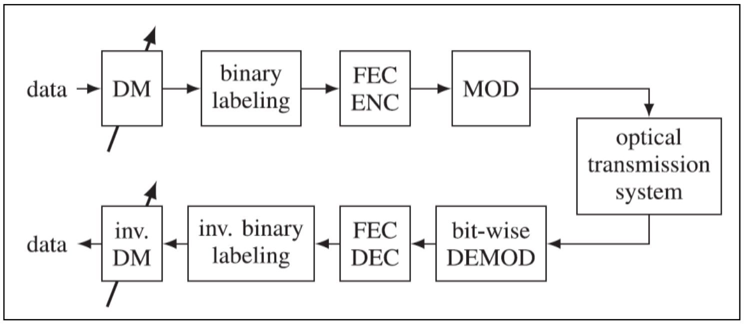

Buchali et al., JLT, vol. 32, p. 1599, 2015

The implementation is not trivial, since the FEC encoder should maintain the probability distribution of symbols.

- DM (distribution matcher): block that converts an input stream of bits uniformly distributed into an output stream of QAM symbols with the desired distribution

Flexibility

- The constellation entropy (or, equivalently, the net data rate) can be changed by changing the value of the parameter λ → high flexibility

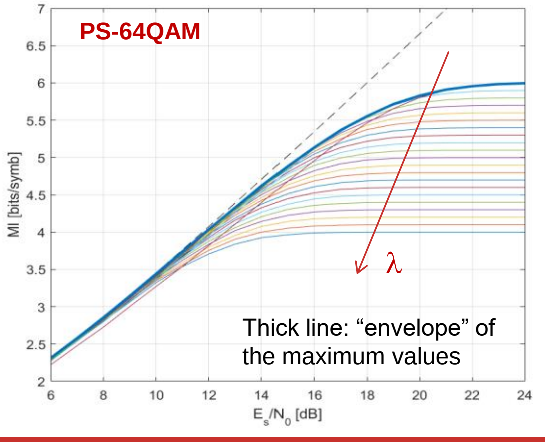

- Each curve corresponds to a different value of λ.
- Shaping reduces the maximum achievable mutual information (or, equivalently, transmit rate), represented by the MI floor for high values of SNR.
- This value corresponds to the constellation entropy:

$$H(C) = -\sum_i P(a_i)\log_2 P(a_i)$$

Flexibility

- The constellation entropy (or, equivalently, the net data rate) can be changed by changing the value of the parameter λ → high flexibility

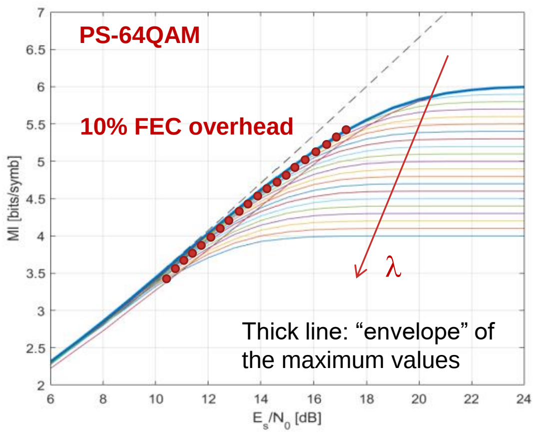

- Each curve corresponds to a different value of λ.
- Shaping reduces the maximum achievable mutual information (or, equivalently, transmit rate), represented by the MI floor for high values of SNR.
- This value corresponds to the constellation entropy:

$$H(C) = -\sum_i P(a_i)\log_2 P(a_i)$$

Ultimate achievable performance

- The optimum value of λ depends on the SNR. The performance of the PS constellations optimized for each value of SNR are shown as blue lines in the below plot:

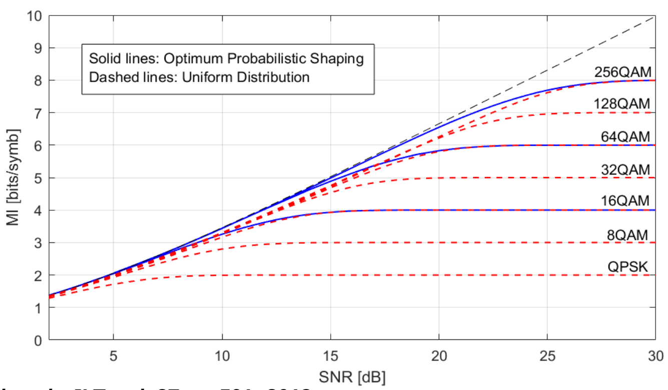

- The gain of PS constellations w.r.t. uniformly-distributed constellations is maximum for mid-values of SNR, then it gets to zero when the MI gets close to the constellation entropy

Pilori et al., JLT, vol. 37, p. 501, 2018

Experimental setup

Symbol rate: 16 Gbaud

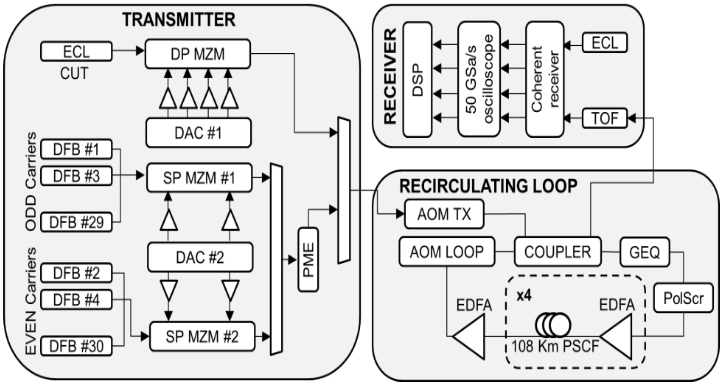

Link parameters.	
EDFAs noise figure	5.2 dB
Chromatic dispersion	20.17 ps/(nm·km)
Non-linearity coefficient	0.75 $W^{-1}\cdot km^{-1}$
Fiber attenuation	0.16 db/km
Total span loss	18 dB

Pilori et al., JLT, vol. 37, 2018

PS-64QAM symbol probabilities

- Graphical illustration of the four employed probability distributions for PS-64QAM.

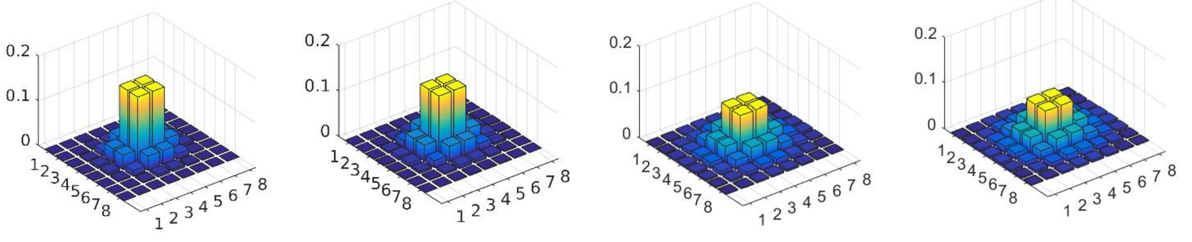

H(P) = 4 bits/symb	H(P)=4.33 bits/symb	H(P)= 5 bits/symb	H(P)=5.17 bits/symb
Same entropy as 16QAM	Same FEC rate as 16QAM	Same entropy as 32QAM	Same FEC rate as 32QAM

Performance after long-haul propagation

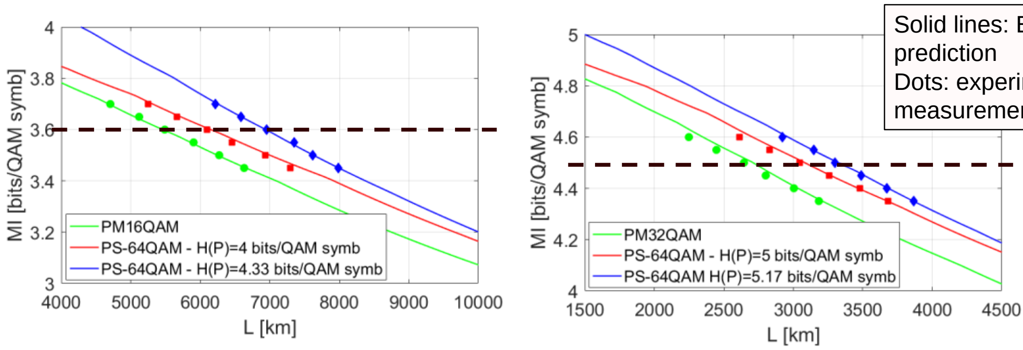

Solid lines: EGN model prediction
Dots: experimental measurements.

- The percentage of **reach increase** w.r.t. uniform 16QAM is between **10% and 25%** at MI=3.6 bits/QAM symb. The percentage of reach increase w.r.t. uniform 32QAM is between **15% and 25%** at MI=4.5 bits/QAM symb.
- The sensitivity gain translated in an equivalent reach gain, without any significant nonlinearity penalty for the PS constellations.

5) Modulation format independent DSP algorithms

DSP functions

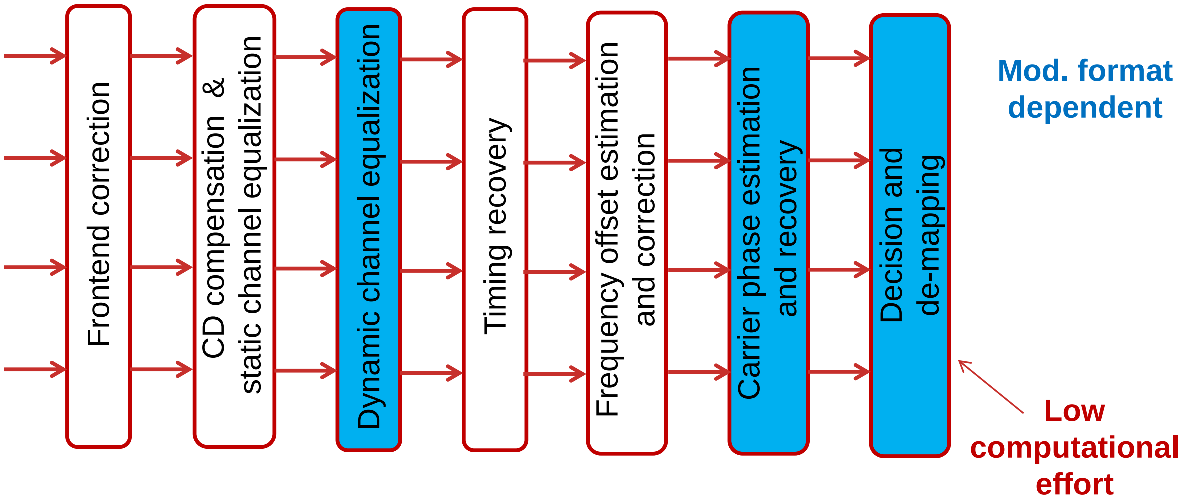

Format-independent adaptive equalizer and CPE

- Popular blind adaptive equalizers update strategies are matched to the specific modulation format. ***Savory, JSTQE, vol. 16, p. 1164, 2010*** ***Millar et al., Opt. Exp., vol. 19, p. 8533, 2011***
- Algorithms for carrier phase recovery which are suitable for arbitrary PM-mQAM formats are extremely complex for high-cardinality constellations. ***Pfau et al., JLT, vol. 27, p.3614, 2009*** ***Zhou, PTL, vol. 22, p. 1051, 2010.***
- Reasonable way to a cost-efficient and format-independent flexible transceiver implementation: **data-aided algorithms**, based on the use of **pilot tones** or **pilot sequences** that are inserted in the payload at the transmitter → additional overhead **Fischer, JLT, vol. 32, p. 2886, 2014.**
  - At the receiver, the pilot information is evaluated independently of the payload and its modulation format.

Pilot tones based DSP

- Pilot tones: continuous wave tones inserted in a gap of the payload spectrum, e.g. they can be inserted between two adjacent channels or at the middle of MSC spectrum.
- They can be used to track time-continuous effects like polarization rotations, frequency offset variations and phase noise.

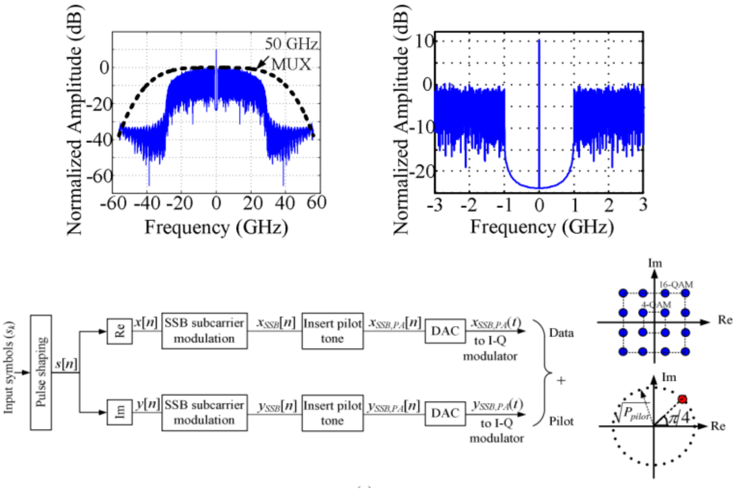

Morsy-Osman et al., Opt. Exp., vol. 19, p. B329, 2011

Pilot sequences based DSP

- Pilot sequences (or training sequences): periodically inserted in time domain at the payload symbol rate.
- They can be used to estimate the channel transfer function and polarization rotations, residual CD, PMD as well as phase noise and frequency offset variations.

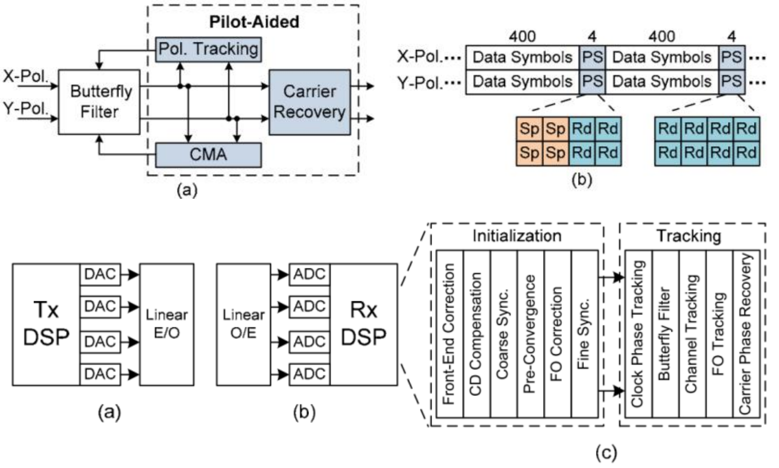

Zhuge et al., Opt. Exp., vol. 22, p. 2278, 2014

Summary

- Advanced modulation format and digital signal processing techniques that can be used to increase the capacity and/or the reach of optical transmission systems, as well as the flexibility of optical transceivers, have been reviewed.

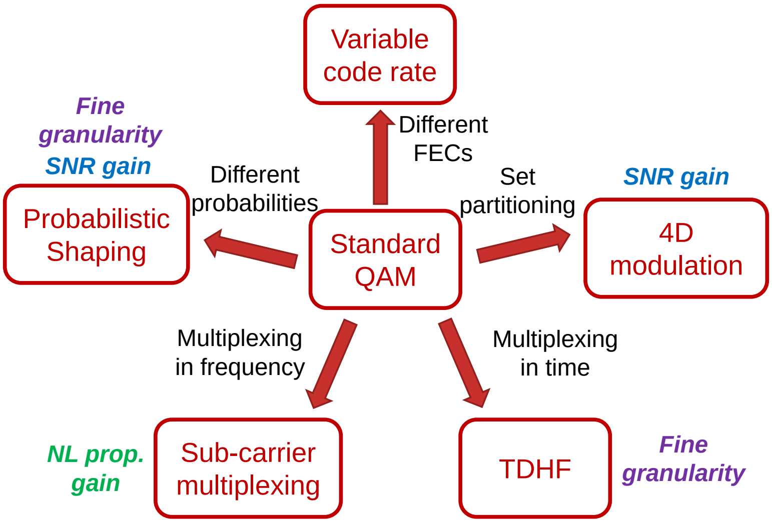

References

References – Flexible transceivers

- K. Roberts and C. Laperle, "Flexible transceivers," ECOC 2012, paper We.3.A.3
- B.T. Teipen, M. Eiselt, K. Grobe, J.-P. Elbers, "Adaptive Data Rates for Flexible Transceivers in Optical Networks," Journal of Networks, vol. 7, no. 5, pp. 776–782, 2012.
- A. Napoli et al., "On the next generation bandwidth variable transponders for future flexible optical systems," European Conference on Networks and Communications (EuCNC), Bologna, 2014.
- K. Roberts et al., "High capacity transport - 100G and beyond," J. Lightwave Technol., vol. 33, no. 3, pp. 563–578, 2015.
- D. A. Morero et al., "Design tradeoffs and challenges in practical coherent optical transceiver implementations," J. Lightwave Technol., vol. 34, no. 1, pp. 121–136, 2016.
- K. Roberts, Q. Zhuge, I. Monga, S. Gareau, C. Laperle, "Beyond 100 Gb/s: Capacity, Flexibility, and Network Optimization," J. Opt. Commun. Netw., vol. 9, no. 4, pp. C12–C24, 2017.
- X. Zhou et al., "Flexible Transceivers: Extracting More Capacity from Elastic Meshed Optical Networks," Asia Communications and Photonics Conference, paper S4C.1, 2017.

References – Adaptive code rate

- G.-H. Gho and J. M. Kahn, "Rate-adaptive modulation and coding for optical fiber transmission systems," J. Lightw. Technol., vol. 30, no. 12, pp. 1818–1828, 2012.
- M. Arabaci, I. B. Djordjevic, L. Xu, and T. Wang, "Nonbinary LDPC-coded modulation for rate-adaptive optical fiber communication without bandwidth expansion," IEEE Photon. Technol. Lett., vol. 24, no. 16,pp. 1402–1404, 2012.
- D. A. A. Mello et al., "Optical networking with variable-code-rate transceivers," J. Lightwave Technol., vol. 32, no. 2, pp. 257–266, Jan. 2014.
- A. Alvarado, D. J. Ives, S. J. Savory, and P. Bayvel, "On the impact of optimal modulation and FEC overhead on future optical networks," J. Lightwave Technol., vol. 34, no. 9, pp. 2339–2352, 2016.
- A. L. N. Souza et al., "Parameter selection in optical networks with variable-code-rate superchannels," J. Optical Comm. Netw., vol. 8, no. 7, pp. A152–A161, 2016.
- D. J. Ives, P. Wright, A. Lord, and S. J. Savory, "Using 25 GbE client rates to access the gains of adaptive bit- and code-rate networking," J. Opt. Commun. Netw., vol. 8, no. 7, pp. A86–A91, 2016.

References – Multi-dimensional formats

- E. Agrell and M. Karlsson, “Power-efficient modulation formats in coherent transmission systems,” J. Lightw. Technol., vol. 27, no. 22, pp. 5115–5126, 2009.
- H. Sun et al., “Comparison of two modulation formats at spectral efficiency of 5 bits/dual-pol symbol,” ECOC 2013, paper Th.2.D.3.
- R. Rios-Muller et al., “Experimental comparison between hybrid-QPSK/8QAM and 4D-32SP-16QAM formats at 31.2 GBaud using Nyquist pulse shaping,” ECOC 2013, paper Th.2.D.2.
- J. Renaudier et al., “Experimental transmission of Nyquist pulse shaped 4-D coded modulation using dual polarization 16QAM set-partitioning schemes at 28 Gbaud,” OFC 2013, paper OTu3B.1.
- A. D. Shiner et al., "Demonstration of an 8-dimensional modulation format with reduced inter-channel nonlinearities in a polarization multiplexed coherent system," Opt. Express, vol. 22, no. 17, pp. 20366–20374, 2014.
- D. S. Millar et al., “High-dimensional modulation for coherent optical communications systems,” Opt. Express, vol. 22, no. 7, pp. 8798–8812, 2014.
- J. K. Fischer, S. Alreesh et al., “Bandwidth-variable transceivers based on four-dimensional modulation formats,” J. Lightw. Technol., vol. 32, no. 16, pp. 2886–2895, 2014.

References – Digital subcarrier multiplexing

- M. Qiu, Q. Zhuge et al., “Digital subcarrier multiplexing for fiber nonlinearity mitigation in coherent optical communication systems,” Opt. Express, vol. 22, n. 15, pp. 18770–18777, 2014.
- Q. Zhuge et al., “Terabit bandwidth-adaptive transmission using low-complexity format-transparent digital signal processing, ” Opt. Express, vol. 22, no. 3, pp. 2278–2288, 2014
- P. Poggiolini et al., “Analytical and experimental results on system maximum reach increase through symbol rate optimization,” J. Lightw. Technol., vol. 34, n. 8, pp. 1872-1885, 2016.
- T. Rahman, D. Rafique et al., “Digital subcarrier multiplexed hybrid QAM for data-rate flexibility and ROADM filtering tolerance,” OFC 2016, paper Tu3K.5.
- X. Meng, Q. Zhuge et al., “Filtering Tolerant Digital Subcarrier Multiplexing System with Flexible Bit and Power Loading,” OFC 2017, paper W4A.7.

References – Time-domain hybrid formats

- X. Zhou et al., "4000 km transmission of 50 GHz spaced, 10 × 494.85-Gb/s hybrid 32–64 QAM using cascaded equalization and training-assisted phase recovery," OFC 2012, paper PDP5C.6.
- Q. Zhuge et al., "Spectral efficiency-adaptive optical transmission using time domain hybrid QAM for agile optical networks," J. Lightw. Technol., vol. 31, n. 15, pp. 2621–2628, 2013.
- X. Zhou, L. E. Nelson and P. Magill, "Rate-adaptable optics for next generation long-haul transport networks," IEEE Communications Magazine, vol. 51, no. 3, pp. 41–49, 2013.
- V. Curri et al. "Time-Division Hybrid Modulation Formats: Tx Operation Strategies and Countermeasures to Nonlinear Propagation," OFC 2014, paper Tu3A.2.
- F. P. Guiomar, et al., "Hybrid modulation formats enabling elastic fixed-grid optical networks," J. Opt. Commun. Netw., vol. 8, n.7, pp. A92–A100, 2016.

References – Probabilistic shaping

- M.P. Yankov et al., "Constellation shaping for fiber-optic channels with QAM and high spectral effciency," IEEE Photon. Technol. Lett., vol. 26, no. 23, pp. 2407–2410, 2014.
- F. Buchali et al., "Rate adaptation and reach increase by probabilistically shaped 64-QAM: An experimental demonstration," J. Lightw. Technol., vol. 34, no. 7, pp. 1599–1609, 2016.
- F.R. Kschischang et al., "Probabilistic 16-QAM Shaping in WDM Systems," J. Lightw. Technol., vol. 34, no. 18, pp. 4285–4292, 2016.
- S. Chandrasekhar et al., "High-spectral-efficiency transmission of PDM 256-QAM with Parallel Probabilistic Shaping at Record Rate-Reach Trade-offs", ECOC 2016, paper. Th.3.C.1.
- F.P. Guiomar et al., "Comparing Different Options for Flexible Networking: Probabilistic Shaping vs. Hybrid Subcarrier Modulation," ECOC 2017, paper Th1.E.3.
- D. Pilori, G. Bosco and C. Fludger, "Impact of finite-resolution DAC and ADC on probabilistically-shaped QAM constellations," IEEE Photonics Conference (IPC), pp. 433–434.
- D. Pilori, L. Bertignono, A. Nespola, F. Forghieri and G. Bosco, "Comparison of Probabilistically Shaped 64QAM with Lower-Cardinality Uniform Constellations in Long-Haul Optical Systems," J. Lightwave Technol., vol.37, no. 2, pp. 501–509, 2018.

References – Tx DSP

- S. J. Savory, “Optimum electronic dispersion compensation strategies for nonlinear transmission,” Electronics Letters, vol. 42, no. 7, pp. 407–408, 2006
- Y. Kamio et al., “Pre-equalization for 10 Gsymbol/s 16-QAM in a vector modulator,” in Proc. IEEE/LEOS Summer Top. Meet., 2008, paper MC1.2.
- A. Ghazisaeidi, J. Renaudier, M. Salsi, P. Tran, G. Charlet and S. Bigo, “System benefits of digital dispersion pre-compensation for non-dispersion-managed PDM-WDM transmission,” ECOC 2013, paper We.4.D.4.
- D. Rafique, T. Rahman, A. Napoli and B. Spinnler, “Digital Pre-Emphasis in Optical Communication Systems: On the Nonlinear Performance,” J. Lightwave Technol., vol. 33, no. 1, pp. 140–150, 2015.
- P. W. Berenguer et al., “Nonlinear Digital Pre-distortion of Transmitter Components,” in Journal of Lightwave Technology, vol. 34, no. 8, pp. 1739–1745, 2016.
- G. Khanna et al., “A Robust Adaptive Pre-Distortion Method for Optical Communication Transmitters,” IEEE Photon. Technol. Lett., vol. 28, no. 7, pp. 752–755, 2016.

References – Rx DSP

- S.J. Savory, “Digital filters for coherent optical receivers," Opt. Exp., vol. 16, no. 2, pp. 804-817, 2008
- T. Pfau, S. Hoffmann and R. Noe, “Hardware-Efficient Coherent Digital Receiver Concept With Feedforward Carrier Recovery for M -QAM Constellations,” J. Lightwave Technol., vol. 27, no. 8, pp. 989-999, 2009.
- M. Kuschnerov et al., “DSP for coherent single-carrier receivers,” J. Lightw. Technol., vol. 27, no. 16, pp. 3614–3622, 2009.
- S. J. Savory, “Digital coherent optical receivers: Algorithms and subsystems, ” IEEE J. Sel. Top. Quantum Electron., vol. 16, no. 5, pp. 1164 – 1179, 2010.
- A. Leven, N. Kaneda, and S. Corteselli, “Real-time implementation of digital signal processing for coherent optical digital communication systems,” IEEE J. Sel. Top. Quantum Electron., vol. 16, no. 5, pp. 1227–1234, 2010.
- X. Zhou, “An improved feed-forward carrier recovery algorithm for coherent receivers with M-QAM modulation format,” IEEE Photon. Technol. Lett., vol. 22, no. 14, pp. 1051–1053, 2010.
- G. Bosco et al. “Impact of the transmitter IQ-skew in multi-subcarrier coherent optical systems,” OFC 2016, paper W4A.5.

References – Rx DSP for flexible transceivers

- M. Morsy-Osman et al., "Joint mitigation of laser phase noise and fiber nonlinearity for polarization-multiplexed QPSK and 16-QAM coherent transmission systems," Opt. Express, vol 19, no. 26, pp. B329-B336, 2011.
- J. K. Fischer et al., "Bandwidth-variable transceivers based on four-dimensional modulation formats," J. Lightw. Technol. , vol. 32, n. 16, pp. 2886 – 2895, 2014.
- Q. Zhuge et al., "Terabit bandwidth-adaptive transmission using low-complexity format-transparent digital signal processing," Opt. Express, vol. 22, no. 3, pp. 2278–2288, 2014.
- A. P. T. Lau et al., "Advanced DSP techniques enabling high spectral efficiency and flexible transmissions: Toward elastic optical networks," IEEE Signal Process. Mag., vol. 31, no. 2, pp. 82–92, 2014.
- X. Zhou and L. Nelson, "Advanced DSP for 400 Gb/s and Beyond Optical Networks," J. Lightwave Technol., vol. 32, no. 16, pp. 2716–2725, 2014.
- X. Liu, S. Chandrasekhar, P. J. Winzer, "Digital Signal Processing Techniques Enabling Multi-Tb/s Superchannel Transmission: An overview of recent advances in DSP-enabled superchannels," IEEE Signal Processing Magazine, vol. 31, no. 2, pp. 16–24, 2014.
- R. Elschner, F. Frey, C. Schmidt-Langhorst, J. K. Fischer, and C. Schubert, "Data-Aided DSP for Flexible Transceivers," Advanced Photonics for Communications 2014, OSA Technical Digest, paper SW1C.1.

Other References

- G. Bosco, V. Curri, A. Carena, P. Poggiolini, and F. Forghieri, "On the performance of Nyquist-WDM terabit superchannels based on PM-BPSK, PM-QPSK, PM-8QAM or PM-16QAM subcarriers," J. Lightw. Technol., vol. 29, no. 1, pp. 53–61, 2011.
- P. J. Winzer, "High-spectral-efficiency optical modulation formats," J. Lightw. Technol., vol. 30, no. 24, pp. 3824–3835, Dec. 2012.
- C. Laperle and M. O ' Sullivan, "Advances in high-speed DACs, ADCs, and DSP for optical coherent transceivers, " J. Lightwave Technol., vol. 32, no. 4, pp. 629–643, 2014
- A. Nespola et al., "1306-km 20x124.8-Gb/s PM-64QAM Transmission over PSCF with Net SEDP 11,300 (b·km)/s/Hz using 1.15 samp/symb DAC," Opt. Express, vol. 22, no. 1, pp. 1796–1805, 2014.
- P. Poggiolini et al., "A simple and effective closed-form GN model correction formula accounting for signal non-gaussian distribution," J. Lightw. Technol., vol. 33, no. 2, pp. 459–473, 2015.
- P.J. Winzer, D.T. Neilson, "From Scaling Disparities to Integrated Parallelism: A Decathlon for a Decade", J. Lightwave Technol., vol. 35, no. 5, pp. 1099–1115, 2017.
- P. Poggiolini and Y. Jiang, "Recent Advances in the Modeling of the Impact of Non-Linear Fiber Propagation Effects on Uncompensated Coherent Transmission Systems", J. Lightwave Technol., vol. 35, no.3, pp. 458–480, 2017.